Some recent aspects of unimolecular gas phase ion chemistry

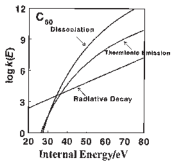

Chava Lifshitz*

Department of Physical Chemistry and The Farkas Center for Light Induced Processes, The Hebrew University, Jerusalem 91904, Israel

Received 13th December 2000
First published as an Advance Article on the web 11th April 2001

Unimolecular reactions in the gas phase have been known for nearly a century. Unimolecular ionic reactions form the basis for mass spectrometry. This review article covers three major aspects: (1) Activation of unimolecular reactions by ambient blackbody radiation and the resultant work on biomolecules. (2) The definition of activated complex parameters through RRKM calculations on *ab initio* potential energy surfaces. (3) Competing decay mechanisms of large hot carbon cluster ions—radiative decay and thermionic emission.

1 Experimental

A molecule can undergo dissociation or isomerization in the gas phase in what has been termed a unimolecular reaction. Unimolecular reactions have been known since the beginning of last century.[1,2] Unimolecular fragmentations of gas phase ions form the basis for analysis by mass spectrometry.

At the cornerstone of chemical kinetics stands the Arrhenius equation,[3] established in 1889, already known when the mechanism of unimolecular reactions was discussed in the early years of the 20th century.[1,2] It established the temperature dependence of reaction rate constants $k(T)$ in terms of activation parameters—an activation energy E_a and a pre-exponential factor A,

$$k(T) = A \exp[-E_a/k_BT] \tag{1}$$

where k_B is what we now know as Boltzmann's constant and the temperature T is defined by the Maxwell–Boltzmann energy distribution. Gas phase ions are normally formed under the very low-pressure conditions prevailing in mass spectrometer ion sources and the definition of a temperature is problematic since thermal equilibrium is not established through collisions.

The present review is devoted to a brief discussion of three aspects of unimolecular reactions of gas phase ions advanced recently. For a reaction to take place, the reactant molecule has to surmount an activation barrier. This means in turn that the molecule has to acquire internal energy. The first aspect to be discussed involves the activation of unimolecular reactions by ambient blackbody radiation, a method called BIRD (Blackbody Infra-Red Dissociation). This method has been particularly useful for large biomolecules whose analysis by mass spectrometry is now at the center of attention. It leads to reliable activation parameters—activation energies and pre-exponential factors—for the characteristic reactions of these molecules, whose temperatures are well defined even under extremely low ion source pressures.

A considerable amount of experimental effort concerning unimolecular reactions of gas phase ions has been devoted to energy-selected systems.[4] All detailed statistical theories of unimolecular reactions begin with the calculation of $k(E)$, the rate constant as a function of the internal energy, E (called the 'microcanonical' rate constant). The Rice–Ramsperger–Kassel Marcus/quasi-equilibrium theory, RRKM/QET, assumes the existence of a transition state. The expression for $k(E)$ is given by,[4]

$$k(E) = \frac{\sigma N^{\#}(E - E_0)}{h\rho(E)} \tag{2}$$

where E_0 is the critical energy of activation (E_0 is not necessarily exactly equal to the Arrhenius activation energy E_a), $\rho(E)$ is the density of vibrational states at the energy E, $N^{\#}(E - E_0)$ is the sum of the vibrational states from 0 to $E - E_0$ in the transition state, h is Planck's constant, and σ is the reaction path degeneracy. Theoretical modeling of energy selected experimental results using eqn. (2) requires knowing the heights of activation barriers and the vibrational frequencies of the reactant and of the transition state. The second aspect of recent research that will be discussed in this review is related to the determination of activation barrier heights, as well as reactant

Chava Lifshitz was born (née Eva Wolf) in Vienna, Austria in 1936 and immigrated to Israel in 1938. She studied chemistry at The Hebrew University of Jerusalem where she obtained her PhD in radiation chemistry with Professor Gabriel Stein in 1961. She worked as a postdoctoral fellow (1961–1963) at Cornell University with Professor Franklin A. Long on mass spectrometry and unimolecular fragmentations of polyatomic ions with application of RRKM/QET. She returned to The Department of Physical Chemistry of The Hebrew University in 1963 as a lecturer, became full professor in 1976 and was awarded the Archie and Marjorie Sherman chair in Chemistry established in 1990. She was a visiting scientist at several institutes, including Argonne National Laboratory in 1965 working on VUV photoionization mass spectrometry with Drs Chupka and Berkowitz. She was a visiting scientist at Cornell University in 1969 working on RRKM/QET of large species with Professor Fred McLafferty, and at Wright Patterson Air Force Base, Ohio in 1969–1970 and 1972 working on ion–molecule reactions and tandem mass spectrometry with Dr Tom Tiernan. She was chairperson of the Chemistry Studies Division (1972–1976) and of The Institute of Chemistry (1994–1997) at The Hebrew University. Her major research interests are mass spectrometry, gas phase ion chemistry, reaction dynamics, photoionization, clusters, fullerenes and small biomolecules. She is a member of editorial advisory boards of several of the major mass spectrometry journals.

This journal is © The Royal Society of Chemistry 2001

and transition state frequencies by recently advanced methods of computational chemistry. This approach has considerably reduced the number of free parameters required to model energy-selected experimental data through calculations of rate/energy dependences, $k(E)$.

Clusters are species that possess a repetitive unit such as an atom or a molecule. They are considered to bridge the gap between isolated species in the gas phase and bulk matter. A particularly interesting group of clusters that are bound by strong covalent bonds are the carbon clusters including the fullerenes. Hot fullerenes, *e.g.* C_{60} ('Buckyball'), can undergo cooling processes—blackbody-like radiative decay in the visible and thermionic emission—in competition with dissociation. Blackbody radiative decay and thermionic emission are well-known bulk phenomena. The third topic of great interest for unimolecular reactions that will be discussed here involves fullerene cooling *via* these competitive unimolecular processes of radiative decay and thermionic emission.

2 Activation of unimolecular reactions by ambient blackbody radiation

Scientists attempting to understand the mechanism of unimolecular reactions in the early days[1,2] were confronted with the following dilemma: in order to acquire the necessary activation energy, the molecules had two alternatives—activation by collision or activation by absorption of radiation. Unimolecular reactions were known to be first-order. Naively, when two molecules collide the reaction should be second-order and an assumed first-order rate should be pressure dependent contrary to experimental observations of that time. That seemed to rule out the collision mechanism. The mechanism put forward to circumvent this problem was that by Perrin[1] who suggested absorption of blackbody photons generated by the surroundings. He concluded that radiation was able to act upon an isolated molecule in vacuum in a manner dependent upon temperature, *i.e.* leading to a reaction rate that follows the Arrhenius equation.[1,5] Perrin's radiation hypothesis was discounted by Langmuir[6] since at the time it was assumed that a single photon, whose energy equals the activation energy, had to be absorbed. The activation energies considered were quite high necessitating the absorption of photons in the ultraviolet. The molecules in question were known not to absorb in this energy range. Furthermore, the radiation density at these wavelengths even at the highest experimental temperatures employed was too low.

Lindemann[2] resolved this dilemma in 1922. According to his mechanism, molecules became energized through bimolecular collisions and the kinetics could still be first-order. Collisional activation and deactivation were assumed to be fast compared to the unimolecular reaction of the activated molecule. As a result, a Maxwell–Boltzmann equilibrium energy distribution is established at the temperature, T. The unimolecular reaction step is rate determining. The well-known Lindemann mechanism has prevailed since 1922 and appears in most text books.[4] It is usually written for neutral species A; in view of our interest in ions an equivalent mechanism is written here for ions as follows.

An ion AB^+ undergoing dissociation can be energized through collisions with a neutral molecule M (M can be a bath gas or possibly neutral AB).

$$AB^+ + M \underset{k_{-1,C}}{\overset{k_{1,C}}{\rightleftharpoons}} [AB^+]^* + M \tag{3}$$

$$[AB^+]^* \xrightarrow{k_d} A^+ + B \tag{4}$$

The steady state assumption is applied to the activated ion $[AB^+]^*$ and an apparent rate constant k_{uni} is obtained for unimolecular decomposition, eqn. (5).

$$k_{uni} = \frac{k_{1,C}k_d[M]}{k_{-1,C}[M] + k_d} \tag{5}$$

The early experiments (on neutral molecules) were run at high pressures such that $k_{-1,C}[M] >> k_d$. In this so-called high-pressure limit

$$k_{uni} = \frac{k_{1,C}k_d}{k_{-1,C}} \tag{6}$$

and overall first-order kinetics prevails.

The low pressures under which ionic reactions are normally studied are not in the high-pressure limit. At intermediate pressures there is the well known fall-off region, in which k_{uni} falls upon reduction of pressure[4] (see Fig. 1). At low pressures the rates should be proportional to pressure, since $k_{-1,C}[M] << k_d$ and therefore

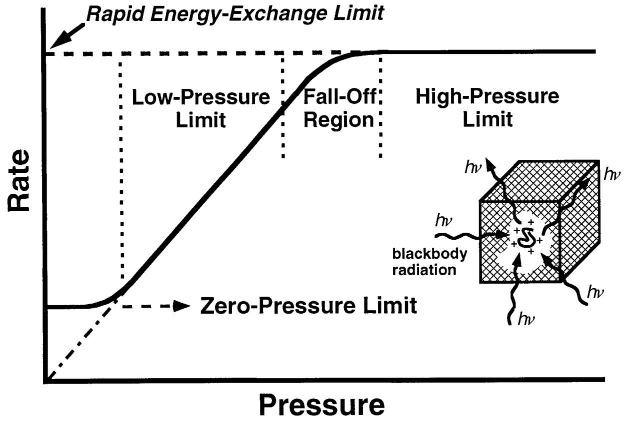

Fig. 1 A modified Lindemann 'fall-off' plot that gives the pressure dependence of the unimolecular dissociation rate constants of small molecules (solid line). At low pressures ($< 10^{-8}$ Torr), the rate constant is non-zero and independent of pressure due to molecular activation by absorption of blackbody radiation. Large molecules such as peptides and DNA are in the rapid energy-exchange (REX) limit indicated by the dashed line. Their rates do not undergo any fall-off but rather remain at the same value as the high-pressure limit even at the very low pressures of $< 10^{-8}$ Torr. This is by virtue of thermal equilibration with blackbody radiation. (Reproduced by permission from *J. Am. Chem. Soc.*, 1996, **118**, 10640. Copyright 1996 American Chemical Society.)

$$k_{uni} = k_{1,C}[M] \tag{7}$$

Extrapolation of thermal reaction rates to zero pressure in the Lindemann mechanism should result in a rate constant of zero.

The radiation hypothesis was considered for many years to be a historical curiosity.[7] This changed dramatically when ionic reactions were studied under the very low pressure conditions ($\sim 10^{-8}$ mbar) and long trapping times (> 1 s) of the Fourier transform ion cyclotron resonance (FT-ICR) ion trap. The first set of reactions to indicate dissociation by absorption of blackbody radiation were those of weakly bound cluster ions such as $H_3O^+L_n$ studied by McMahon and coworkers.[7,8] The loss of a ligand molecule L was observed to occur spontaneously and to be pressure independent. Characteristic results for the dissociation of $H_3O^+[(CH_3)_2O][H_2O]_2$ at two temperatures[7] are presented in Fig. 2. Contrary to the Lindemann mechanism, the ion dissociation rate shows a nonzero intercept at zero pressure of methane bath gas. The radiation hypothesis appeared to be the only possible explanation for a pressure independent means of activation.[7,8] A combination of blackbody radiation-induced and collisional activation mechanisms,[7] eqn. (8), reproduces the experimental results presented in Fig. 2. If k_{abs} is the rate constant for blackbody radiation-induced dissociation and k_f is the collisionally activated rate constant in the low pressure regime, then

$$k_{uni} = k_{abs}[h\nu] + k_f[M] \tag{8}$$

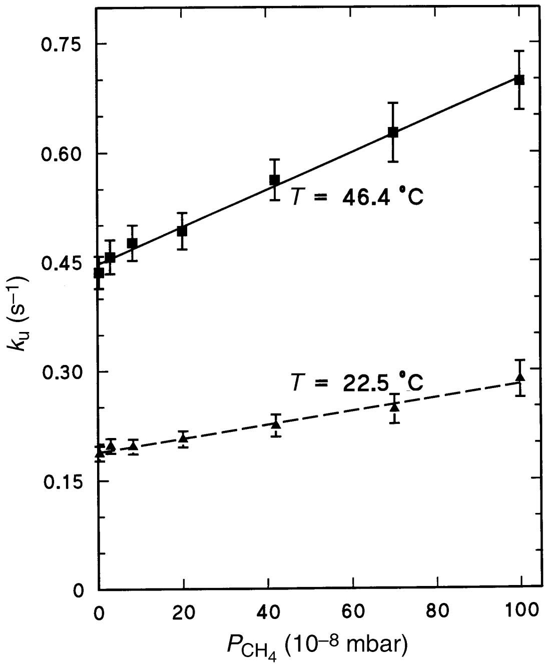

Fig. 2 Dependence of the unimolecular rate of dissociation of the ion $H_3O^+[(CH_3)_2O][H_2O]_2$ (through loss of a water molecule), k_u (= k_{uni}) on pressure P, showing the nonzero intercept at zero pressure of methane bath gas that is due to absorption of blackbody radiation. (Reproduced by permission from *Science*, 1998, **279**, 194. Copyright 1998 American Association for the Advancement of Science.)

A quantitative understanding of the radiation-induced process became possible through the work of Dunbar by analogy with previous low-intensity continuous-wave CO_2 laser dissociation experiments. These experiments had shown that a low-intensity laser driving a reaction by IR multiphoton absorption could be considered as effectively equivalent to a blackbody source.[7] With this analogy came the recognition that the radiation hypothesis was correct with the two following caveats. (a) It is an important mechanism only at very low pressures; (b) absorption is in the infrared and not in the UV as originally suggested.[1,5,6] Unimolecular reactions are thermal reactions, not photochemical reactions. The reactant can equilibrate thermally with the walls of the reaction vessel through collisions or through absorption of radiation.

Analysis of experimental data for small ions such as the proton bound clusters[7,8] requires elaborate modeling[9] since absorption of blackbody photons is the rate-limiting step in the observed overall dissociation process. The characteristic thermal equilibrium Boltzmann distribution of internal energies at the temperature of the experiment is truncated by removal through dissociation of the most energy-rich component of the population.[7]

In the large-ion case the typical unimolecular dissociation rate of the activated ion is slow compared with the rate of energy equilibration with the surroundings by photon exchange. This is because for large ions, *e.g.* biopolymers such as peptides and DNA, the number of oscillators, and hence the number of blackbody photons exchanged with the chamber walls, increases approximately linearly with size. On the other hand, dissociation rates decrease with increasing ion size for a fixed internal energy (this can be verified using eqn. (2)); for ions in thermal equilibrium, the dissociation rate is independent of molecular size for a given dissociation process.[10] Eqn. (3) is replaced by eqn. (9),

$$AB^+ \underset{k_{-1,\text{rad}}}{\overset{k_{1,\text{rad}}}{\rightleftharpoons}} [AB^+]^* \tag{9}$$

where the subscript “rad” denotes the radiative energy transfer rate constants for black body absorption and emission of photons. The large ion case is also called the rapid energy exchange (REX) limit (Fig. 1).[7,10,11] In the REX limit $k_{1,\text{rad}}$, $k_{-1,\text{rad}} >> k_{\text{d}}$ and the measured reaction rates are given by

$$k_{\text{uni}} = \frac{k_{1,\text{rad}} k_{\text{d}}}{k_{-1,\text{rad}}} \tag{10}$$

Dissociation is the rate-limiting step, ions equilibrate with the blackbody radiation field inside the vacuum chamber, and the internal energy distribution of the ions is given by a Boltzmann distribution.

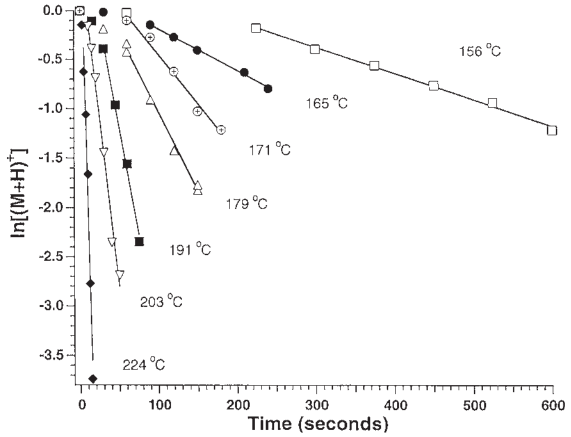

Fig. 3 Data for the dissociation of protonated bradykinin, M + H$^+$, fitted to first order kinetics at the temperatures indicated. The rate constants in order of increasing temperature are 0.0027, 0.0042, 0.013, 0.016, 0.043, 0.068, and 0.32 s^{-1}. Activation is by absorption of blackbody radiation. (Reproduced with permission from *J. Am. Chem. Soc.*, 1996, **118**, 7178. Copyright 1996 American Chemical Society.)

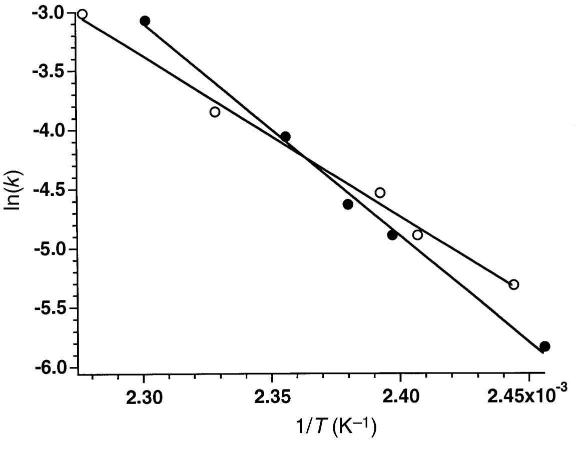

Fig. 4 Arrhenius plots for dissociations of multiply protonated ubiquitin activated by absorption of blackbody radiation. (○) ubiquitin quintuply protonated, ubiquitin^{5+}, undergoing water and/or ammonia elimination; (●) ubiquitin with eleven protons, ubiquitin^{11+}, undergoing cleavage of the amide backbone. (Reproduced with permission from *J. Am. Chem. Soc.*, 1996, **118**, 10640. Copyright 1996 American Chemical Society.)

In the REX limit it is possible to obtain Arrhenius activation parameters, in the complete absence of collisions, equal to those in the high-pressure limit (Fig. 1).[10,11] This provides a route to measuring accurate dissociation energetics for large ions. The dissociation rate constant for the singly protonated nonapeptide bradykinin (Arg-Pro-Pro-Gly-Phe-Ser-Pro-Phe-Arg) was found to be pressure independent within a pressure range of 5 × 10^{-9} – 5 × 10^{-7} Torr. Fig. 3 represents experimental dissociation data at several temperatures fitted to unimolecular kinetics. The major fragment is due to elimination of ammonia with an activation energy E_a = 1.3 eV (125.4 kJ mol^{-1}) and a pre-exponential factor A = 10^{12} s^{-1}.[12] Fig. 4 represents the Arrhenius plot for dissociation of two charge states, 5+ and 11+, of ubiquitin, a protein consisting of 76 amino acid residues. The

11^+ ion undergoes cleavage of the amide backbone with high activation parameters,[10] E_a = 1.6 eV (154.4 kJ mol^{-1}) and $A = 10^{17}$ s^{-1}, demonstrating a 'loose' transition state,[4] *i.e.* a loosening up of the structure upon dissociation. On the other hand, the 5^+ ion undergoes water and/or ammonia elimination with low activation parameters, E_a = 1.2 eV (115.8 kJ mol^{-1}) and $A = 10^{12}$ s^{-1}, *via* a more 'tight' transition state.[10] Activation energies for dissociation of double strand oligonucleotide anions have led[13] to evidence for Watson–Crick base pairing *in vacuo*. The new method of blackbody infrared radiative dissociation (BIRD)[12] thus provides highly interesting information about dissociation energetics and mechanisms of sequence-specific bond cleavages in peptides, proteins and DNA.[11]

3 Calculating reaction kinetics on *ab initio* potential energy surfaces

The dissociation of ions has been analyzed with the aid of statistical theories of unimolecular decay. The dissociation rate constant of an energy-selected ion given by eqn. (2) is determined with programs for evaluating the sums and densities of vibrational states.[4] The major problem in the past has been the selection of vibrational frequencies for the molecular ion and the transition state (TS).[14] This has now been overcome with the development of computational chemistry through *ab initio* MO (molecular orbital) methods[15] (*ab initio* means 'from first principles' and uses the Schrödinger equation) and density functional theory (DFT) calculations.[16] As a result, the only remaining variable is the activation energy, E_0.[14]

An interesting property of transition states is their degree of 'tightness' or 'looseness'. Simple bond cleavages are characterized by loose transition states whereas reactions involving rearrangements lead to tight transition states. The former reactions have usually no reverse activation energies whereas the latter possess substantial activation barriers for the reverse reactions. As noted in the previous section, low Arrhenius pre-exponential A factors for thermal unimolecular reactions correspond to tight transition states, whereas loose transition states lead to high A factors. The activation entropy is the molar entropy of the transition state minus the molar entropy of the reactant, $\Delta S^\# = S^\# - S$. It is a convenient parameter[4] that characterizes the nature of the transition state. A positive $\Delta S^\#$ corresponds to a loose transition state whereas a negative $\Delta S^\#$ corresponds to a tight transition state. The activation entropy is related to the Arrhenius pre-exponential factor *via* eqn. (11),

$$A = \mathrm{e}\frac{k_B T}{h}\exp(\Delta S^\# / R) \qquad (11)$$

where R is the gas constant. In energy selected systems the degree of tightness of the transition-state is judged by its vibrational frequencies. $\Delta S^\#$ is calculated from the frequencies of the reactant and transition state through well-known equations from statistical thermodynamics.[4]

A combined MO and RRKM analysis of energy-selected dimethylformamide cations, $\mathbf{(CH_3)_2NCHO^{\cdot +}}$, was carried out.[17] The ion undergoes two parallel reactions: loss of CHO· and of CH_3·. The vibrational frequencies for the molecular ion and the two transition states were obtained from *ab initio* MO calculations whereas the activation energies were treated as adjustable parameters. Very nice agreement was obtained between calculated and experimental $k(E)$ dependences[17] (Fig. 5). One would have naively assumed that these reactions are simple bond cleavages. The RRKM analysis leading to the computed $k(E)$ dependences (Fig. 5) showed that the apparently simple dissociation reactions proceed *via* substantial reverse activation energies and tight transition states. They are not simple bond cleavages but rather proceed *via* hidden intramolecular hydrogen atom transfers.

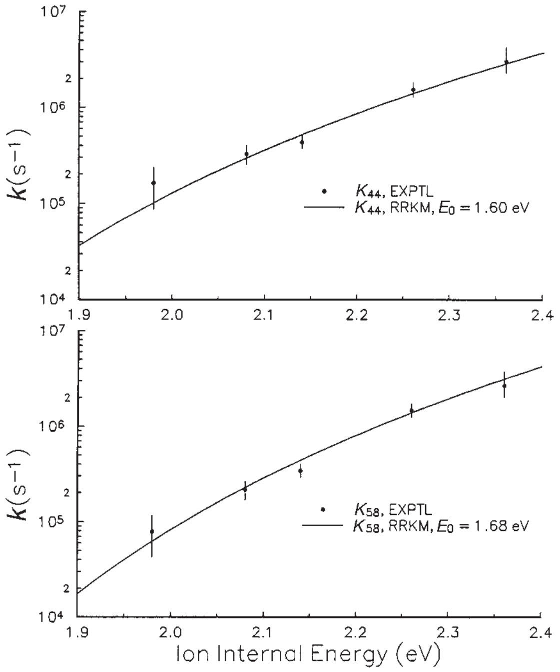

Fig. 5 Experimental and RRKM rate constants as functions of ion internal energy for two parallel reactions of $\mathbf{(CH_3)_2NCHO^{\cdot +}}$, (a) **CHO·** loss leading to an ion with a mass to charge, *m*/*z* ratio of 44 and (b) $\mathbf{CH_3}$**·** loss leading to an ion at *m*/*z* 58. The experimental data are from a technique called Photoelectron-Photoion Coincidence (PEPICO). The theoretical curves were generated using eqn. (2) with frequencies calculated by *ab initio* MO theory and the indicated barrier heights. (Reproduced with permission from *J. Phys. Chem.*, 1993, **97**, 385. Copyright 1993 American Chemical Society.)

In several cases in which the transition state involves the transfer of H· atoms and the transition state energy was calculated by *ab initio* methods, the energy was significantly higher than the experimental dissociation threshold. In these cases quantum mechanical tunneling through the barrier was invoked. RRKM calculations, involving a modification of eqn. (2), in which the hydrogen atom tunnels through the barrier, gave agreement with the experimental observations. These reactions include the elimination of methane from acetone ions,[18] the loss of HCl from energy-selected ethyl chloride ions,[19] and the H_2 loss reaction from ethane ions.[20]

Recent progress in *ab initio* electronic structure theory has led to the development of methods for the calculation of molecular energies capable of chemical accuracy (1–2 kcal mol^{-1} or better) for small and medium sized molecules. RRKM and *ab initio* MO calculations of unimolecular ionic dissociations have been reviewed in 1996.[14] Additional improvements have been made since then. The hypersurface for rearrangement and dissociation reactions of the methyl formate ion was calculated[21] by so-called G2 *ab initio* MO theory. This hypersurface, having several maxima and minima, was transformed into a simplified two-well one-product model potential energy surface. This enabled RRKM calculations to be carried out[21] that gave good agreement with experimental results. Potential energy profiles for ionic reactions can now be computed with some degree of certainty, although there are still uncertainties in calculated energy barrier heights.

Our own group was involved in two endeavors of this kind. In the first,[22] the energetics of the $\mathbf{C_{10}H_8}^{\cdot +}$ – naphthalene$^{\cdot +}$/azulene$^{\cdot +}$ monocation isomerization were calculated by DFT as well as by a more advanced 'coupled cluster' method. The isomerization barriers between naphthalene$^{\cdot +}$ and azulene$^{\cdot +}$ were found to be lower than the lowest corresponding dissociation limits, namely those for H· loss and acetylene elimination. This computational result was checked through measurements of the microcanonical rate constants $k(E)$ for acetylene elimination from naphthalene and azulene cation radicals through time resolved photodissociation (TRPD) of energy-selected ions. Molecular ions are photoexcited by a laser to a well-defined internal energy in TRPD experiments and the measured time resolved appearance signal of the dissociation product ion yields $k(E)$. One defines an absolute energy scale such that the zero of the energy scale corresponds, in the case of the $\mathbf{C_{10}H_8}^{\cdot+}$ isomers, to ten neutral carbon atoms and four neutral H_2 molecules The different internal vibrational energies of the ionic isomers are chosen in the experiment in such a way that their absolute energies are equal. The rates were found equal for the two isomers when measured at the same absolute energy (Fig. 6) and in agreement with RRKM calculations carried out for naphthalene$^{\cdot+}$ using eqn. (2).[23] The complex hypersurface for naphthalene$^{\cdot+}$/azulene$^{\cdot+}$ isomerization and dissociation obtained by DFT computational chemistry[22] was transformed into a simplified two-well one-product model potential energy surface (Fig. 7). Azulene$^{\cdot+}$ undergoes isomerization to naphthalene$^{\cdot+}$ *en route* to acetylene elimination. It samples therefore the naphthalene$^{\cdot+}$ potential well with its relatively high density of vibrational states. It is apparently the exit from this deep potential well with its high density of vibrational states, $\rho(E)$, that is rate determining (see eqn. (2)) causing naphthalene$^{\cdot+}$ and azulene$^{\cdot+}$ to undergo the reaction at the same rate. The experimental observation of equal rates at equal absolute energies for the two ions constitutes proof for isomerization below the dissociation limit.

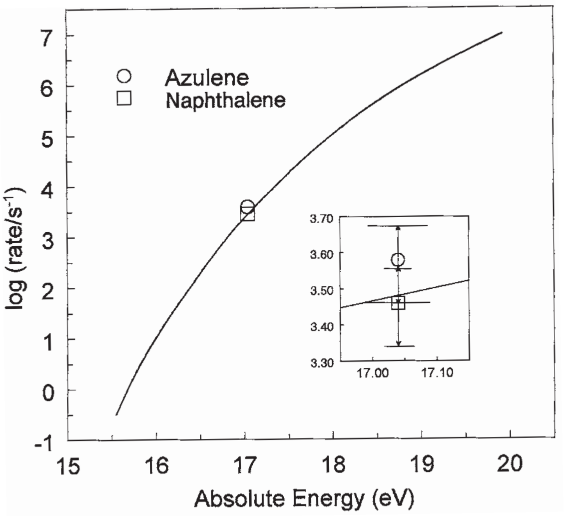

Fig. 6 TRPD experimental values for the rate constants for acetylene loss from naphthalene$^{\cdot+}$ (□) and azulene$^{\cdot+}$ (○). The curve is the RRKM rate-energy curve, known to be in agreement with a set of experimental results for the naphthalene$^{\cdot+}$ ion, plotted as a function of absolute energy. (Reproduced with permission from *J. Phys. Chem. A*, 2000, **104**, 6343. Copyright 2000 American Chemical Society.)

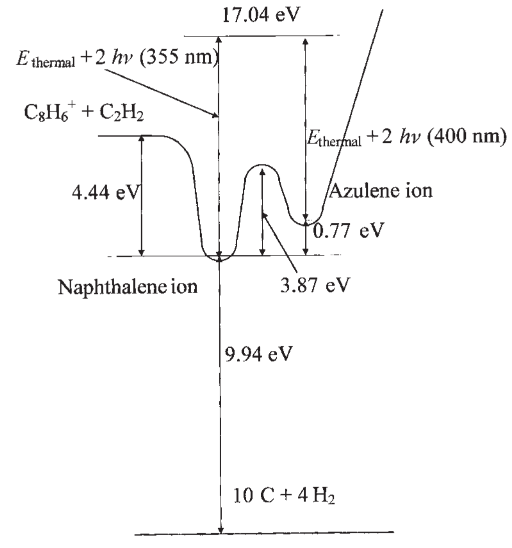

Fig. 7 Schematic potential energy profile for the isomerization and dissociation of the naphthalene$^{\cdot+}$–azulene$^{\cdot+}$ isomer pair. The isomerization barrier is the highest calculated barrier along the isomerization path [22] that corresponds to a norcaradiene$^{\cdot+}$ isomer. Azulene$^{\cdot+}$ is less stable than naphthalene$^{\cdot+}$ by 0.77 eV. The azulene$^{\cdot+}$ and naphthalene$^{\cdot+}$ cations are excited to the same absolute energy of 17.04 eV. This is achieved for azulene$^{\cdot+}$ by absorption of two photons at 400 nm and for naphthalene$^{\cdot+}$ by absorption of two photons at 355 nm. Both ions lead upon acetylene elimination to the same product $C_8H_6^{\cdot+}$ structure, benzocyclobutadiene$^{\cdot+}$. (Reproduced by permission from *J. Phys. Chem. A*, 2000, **104**, 6343. Copyright 2000 American Chemical Society.)

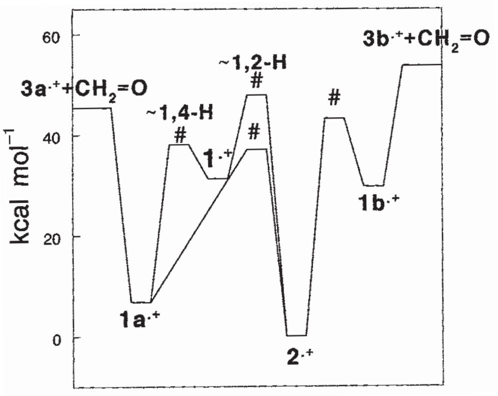

Fig. 8 Potential energy profile for isomerization and dissociation *via* formaldehyde elimination of dimethyl phosphonate and dimethyl phosphite ions, $\mathbf{(CH_3O)_2P(H) = O^{\cdot+}}$, ($\mathbf{1}^{\cdot+}$) and $\mathbf{(CH_3O)_2P\text{-}OH}^{\cdot+}$, ($\mathbf{2}^{\cdot+}$), respectively, at 298 K. These are computational results of *ab initio* electronic structure theory using the CBS-QB3 hybrid empirical correction/pair extrapolation method.[25] The ion $\mathbf{\cdot CH_2O\text{-}(CH_3O)P^+(H)OH}$, ($\mathbf{1a}^{\cdot+}$) and ion ($\mathbf{1b}^{\cdot+}$) are isomeric ions of $\mathbf{1}^{\cdot+}$ and $\mathbf{2}^{\cdot+}$. $\mathbf{(CH_3O)P^{\cdot+}(H)OH}$, ($\mathbf{3a}^{\cdot+}$), and its isomer ($\mathbf{3b}^{\cdot+}$) are the two most stable ionic dissociation products formed upon elimination of CH_2O. The symbol # signifies a transition structure. (Adapted from *Z. Phys. Chem.*, 2000, **215**, 141.)

The second effort was made in the calculation of the rather complex potential energy profile for tautomerization and dissociation of dimethyl phosphonate and dimethyl phosphite ions, $\mathbf{(CH_3O)_2P(H) = O^{\cdot+}}$, ($\mathbf{1}^{\cdot+}$) and $\mathbf{(CH_3O)_2P\text{-}OH}^{\cdot+}$, ($\mathbf{2}^{\cdot+}$) respectively.[24] The calculation of energetics of molecules containing atoms of the second row of the periodic table such as phosphorus are quite demanding. Geometries were calculated at the so-called B3LYP level with an augmented basis set denoted 6-311G(2d,d,p). Energetics were evaluated using the complete basis set (CBS) methods of Petersson and coworkers.[25] Experiments involved photoionization in the VUV and tandem mass spectrometry methods. Theory and experiment yielded a consistent potential energy profile (Fig. 8).[24] Contrary to the naphthalene$^{\cdot+}$–azulene$^{\cdot+}$ isomer pair, the phosphonate$^{\cdot+}$–phosphite$^{\cdot+}$ pair of isomers are separated by a 1,2-H shift barrier that is high in comparison with the lowest dissociation limit leading to formaldehyde elimination. On the other hand the phosphonate ion, $\mathbf{(CH_3O)_2P(H) = O^{\cdot+}}$, ($\mathbf{1}^{\cdot+}$) readily isomerizes *via* a 1,4-H shift to a very stable 'distonic' ion (in which the radical and ion sites are distant from one another), $\mathbf{\cdot CH_2O\text{-}(CH_3O)\text{-}P^+(H)OH}$, ($\mathbf{1a}^{\cdot+}$) and related ion-dipole complexes which serve as precursors for the low energy loss of $CH_2 = O$ and formation of $\mathbf{(CH_3O)P^{\cdot+}(H)OH}$, ($\mathbf{3a}^{\cdot+}$). RRKM calculations have not yet been performed on this complex surface, nor have energy selected measurements of microcanonical rate constants, $k(E)$. However, the state of the art of MO theory is obviously improving and activation energies will not have to be treated as free parameters in RRKM calculations, before long. We affixed ±4 kcal mol^{-1} as a conservative estimate for the uncertainty in computed barrier heights in the phosphonate$^{\cdot+}$–phosphite$^{\cdot+}$ surface.[24]

4 Competing decay mechanisms of large hot ions

Fullerenes have been among the large systems studied in recent years by mass spectrometry and gas phase ion chemistry. It was soon realized that these species differ in their behaviour from small molecules. One major change is the intervention of decay mechanisms other than dissociation. Hot carbon clusters can cool down by several parallel processes including evaporation of neutral fragments (dissociative decay), emission of photons (blackbody-like radiative decay) and electron emission (delayed ionization or 'thermionic emission'). The understanding of the intricate interplay between these various cooling processes although being of great current interest is still in its infancy. Internally (rotationally–vibrationally) hot positive C_{60}^{*+} ions undergo two competing processes (the asterisk denotes internal excitation):

$$C_{60}^{*+} \rightarrow C_{58}^{+} + C_2 \tag{12}$$

$$C_{60}^{*+} \rightarrow C_{60}^{+} + h\nu \tag{13}$$

Internally hot C_{60}^{*} neutrals undergo all three of the following cooling processes:

$$C_{60}^{*} \rightarrow C_{58} + C_2 \tag{14}$$

$$C_{60}^{*} \rightarrow C_{60} + h\nu \tag{15}$$

$$C_{60}^{*} \rightarrow C_{60} + e^{-} \tag{16}$$

The optical emission spectra of laser desorbed neutral C_{60}^{*} were observed[26] to be structureless, demonstrating close similarities to blackbody-like radiation, and could be fitted with the Planck blackbody formula. Photon emission blackbody-like radiative decay [reactions (13) & (15)] and thermionic emission [reaction (16)] are slow RRKM-like unimolecular processes that take place following internal conversion of electronic excitation energy into vibrational energy and following intramolecular vibrational redistribution (IVR). Delayed ionization has been termed thermionic emission signifying the coupling of rovibronic and electronic states in the molecule.[27] Thermionic emission can compete with the evaporation of a C_2 unit from neutral C_{60} because the ionization energy of C_{60} (7.6 eV) is lower than the C_2 binding energy ($\sim$10 eV). Thermionic emission does not compete with C_2 evaporation from the positive ion because the second ionization energy is rather high (11.4 eV).

Radiative cooling rates have been determined experimentally through their competition with C_2 evaporation or electron emission. An estimate of the cooling rate at $T \cong 1800$ K was obtained[28] from observation of the depletion of thermal C_{60}^{*} beams by fragmentation. The dissociation kinetics of neutral C_{60} was used as a thermometric probe. Radiative cooling of C_{60}^{*-} can be followed by thermionic emission as a function of time after injection into a heavy-ion storage ring. In this experiment[29] the electron emission is used as a calibrated thermometer to measure the cooling rate. The advantage of this method is that the electron affinity of C_{60} is very accurately known and the radiative rate can be determined over a range of temperatures. The radiative cooling rate of C_{60}^{*+} can be determined[30] through its competition with C_2 evaporation. The method employs two-electron dissociative ionization of C_{60} at electron energies where the single electron dissociative ionization process does not occur. In the internal energy range (19 ± 3.5) eV ($\sim$ 1800 K) the mean radiative rate is $k_{\mathrm{rad}} = (3.3 \pm 1) \times 10^{2}\ \mathrm{s}^{-1}$. Experimental results are lacking at higher temperatures at which competition with C_2 evaporation from C_{60}^{*+} takes place. Computations were carried[31] out in this energy range, albeit for neutral C_{60}. Two models were employed: (a) calculations based on measured oscillator strengths from absorption spectra of C_{60} and (b) a blackbody model modified for small species. Whether a blackbody model is applicable for the emission of radiation from C_{60} or its ions is controversial. The authors concluded[31] that the oscillator treatment is superior to the blackbody model.

Radiative decay rates deduced between $\sim$3000 and 4000 K (in the range of energies $E \sim$ 40–50 eV) are much higher than originally anticipated since emission is in the visible due to electronic transitions and not in the infrared due to vibrational transitions. Radiative cooling has been demonstrated[32] to suppress the fraction of 'metastable'—internally excited—fullerene ions undergoing C_2 evaporation in the field free region of a time-of-flight (TOF) mass spectrometer (the so-called 'metastable fraction'). Another attribute of unimolecular reactions that is of great value is the kinetic energy released in the center of mass system, as the two products of the dissociation recede from one another. A mass spectrometer called Ion Trap/Reflectron TOF combines an ion trap, in which ions can be trapped for variable times, with a high-resolution fast and sensitive detection TOF instrument. It can be employed to do time resolved measurements—time resolved metastable fractions and time resolved kinetic energy releases. As the ions are trapped for longer times before undergoing ejection into the field-free region of the TOF, the ions that still react in flight will have lower energies and therefore lead to lower metastable fractions and lower kinetic energy releases. Time resolved metastable fractions for C_2 evaporations from C_n^{+} ions were measured and modeled[33,34] using microcanonical dissociative as well as radiative decay rate constants. Dissociative decay is important for C_{60}^{+} at short times but radiative decay is already a strongly contributing factor on the microsecond time scale and becomes the dominant channel at 30 μs as judged from theoretical modeling[35] of time resolved kinetic energy releases.

The transition from direct to delayed ionization has recently been determined experimentally. Either nanosecond or femtosecond laser pulses have been used to ionize fullerenes. For very short laser pulses (25 fs) a direct sequential multiphoton ionization occurs on the timescale of the excitation. The onset of delayed, thermionic electron emission from C_{60} occurs[36] on a timescale of 500–1000 fs. This is the timescale for the coupling of electronic and vibrational excitation. Rate constant calculations for thermionic emission[37] have implicitly assumed statistical behaviour in which the activated molecule is in a state that interconverts rapidly with the full phase space of electronic and vibrational states available. Rate constants become unpredictable[38] unless there is complete energy randomization. In recent calculations[39] the rate energy curves, $k(E)$, for dissociation (C_2 evaporation) and thermionic emission of neutral C_{60} cross one another (Fig. 9) and diverge at high energies. According to the recent model, dissociation is dominant at high energies, although it has a high activation energy, since it has a very loose transition state. The activation parameters used for reactions (14) and (16) in Fig. 9 are: Arrhenius pre-exponential A factors, $A(14) = 8 \times 10^{20}\ \mathrm{s}^{-1}$; $A(16) = 2 \times 10^{16}\ \mathrm{s}^{-1}$; activation energy for reaction (14) (= binding energy) $E_{\mathrm{a}}(14) = 10$ eV; activation energy for reaction (16) (= ionization energy) $E_{\mathrm{a}}(16) = \mathrm{IE}(C_{60}) = 7.6$ eV.

The dissociation mechanism of C_{60} has been studied through *ab initio* quantum-chemical calculations. C_2 elimination is a multiple step process. The last step involves formation of a C_{58} isomer containing a seven-membered ring to which a C_2 'stick' is loosely bound. The C_2 molecule that leaves the fullerene surface is due to a bond shared by a hexagon and a pentagon (5–6 bond). These findings by Scuseria and coworkers formed the basis for a computation[39] of the A factor for reaction (14) by statistical thermodynamics. The value deduced at $k_BT = 0.2$ eV, $A(14) = 8 \times 10^{20}\ \mathrm{s}^{-1}$, is considered to be an upper limit. The C_2 binding energy in C_{60} has been determined by several

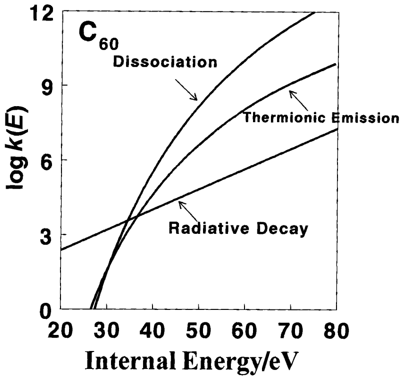

Fig. 9 Microcanonical rate constant, $k(E)$ in s^{-1}, as a function of energy, E in eV, for dissociative decay, radiative decay and thermionic emission of neutral C_{60}, reactions (14), (15) and (16), respectively. The activation parameters for dissociation and thermionic emission are given in the text. The radiative decay rate can be cast in the form: $\log k(E) = 0.082\,E + 0.744$. (Reproduced with permission from *Int. J. Mass Spectrom.*, 2000, **198**, 1. Copyright 2000 Elsevier Science.)

independent methods including high-level DFT calculations to be ≥10 eV. The microcanonical $k(E)$ dependence on energy (Fig. 9) based on $A(14) = 8 \times 10^{20}\ s^{-1}$ and $E_a(14) = 10$ eV was calculated for reaction (14) by RRKM. The microcanonical rate constants for dissociation and thermionic emission of C_{60} have not yet been determined experimentally. The efficiency of thermionic emission has been determined experimentally to reach 2.6%. The model calculations of Fig. 9 lead to a thermionic emission yield of about 2.6% in the range of ~ 10 μs, as required.[39]

5 Summary and conclusions

In this article we have tried to summarize some of the recent advances made in unimolecular gas phase ion chemistry. The technological advances made in experiments enabled many of the new observations. The high vacuum techniques enabled for the first time, after nearly a century, the experimental observation of the Perrin mechanism of activation by absorption of blackbody radiation. The high mass ranges and high mass resolutions available in modern mass spectrometry combined with new methods for evaporation and ionization of clusters and biomolecules revealed hitherto unknown phenomena such as delayed ionization or 'thermionic' emission. Finally, the theoretical modeling of rate–energy dependences while still very strongly dependent on the relatively old ideas of Transition State Theories and RRKM/QET are now combined with the newly developed electronic computational MO theories, *ab initio* and DFT. This combination has nearly completely rendered void the necessity for free parameters.

6 Acknowledgments

This research has been supported by the EU Cluster Cooling Network (HPRN-CT-2000-00026). The Farkas Center is supported by the Minerva Gesellschaft für die Forschung GmbH, München.

7 References

1 J. Perrin, *Ann. Phys.*, 1919, **11**, 5.
2 F. A. Lindemann, *Trans. Faraday Soc.*, 1922, **17**, 598.
3 S. Arrhenius, *Z. Phys. Chem.*, 1889, **4**, 226.
4 T. Baer and W. L. Hase, *Unimolecular Reaction Dynamics; Theory and Experiment,* Oxford University Press, New York – Oxford, 1996.
5 J. Perrin, *Trans. Faraday Soc.*, 1922, **17**, 546.
6 I. Langmuir, *J. Am. Chem. Soc.*, 1920, **42**, 2190.
7 R. C. Dunbar and T. B. McMahon, *Science*, 1998, **279**, 194.
8 D. Thölmann, D. S. Tonner and T. B. McMahon, *J. Phys. Chem.*, 1994, **98**, 2002.
9 R. C. Dunbar, *J. Phys. Chem.*, 1994, **98**, 8705.
10 W. D. Price, P. D. Schnier, R. A. Jockusch, E. F. Strittmatter and E. R. Williams, *J. Am. Chem. Soc.*, 1996, **118**, 10640.
11 W. D. Price and E. R. Williams, *J. Phys. Chem. A*, 1997, **101**, 8844.
12 P. D. Schnier, W. D. Price, R. A. Jockusch and E. R. Williams, *J. Am. Chem. Soc.*, 1996, **118**, 7178.
13 P. D. Schnier, J. S. Klassen, E. F. Strittmatter and E. R. Williams, *J. Am. Chem. Soc.*, 1998, **120**, 9605.
14 P. B. Armentrout and T. Baer, *J. Phys. Chem.*, 1996, **100**, 12866.
15 W. J. Hehre, L. Radom, P. v. R. Schleyer and J. A. Pople, *Ab Initio Molecular Orbital Theory,* Wiley-Interscience, New York, 1986.
16 A. P. Scott and L. Radom, *J. Phys. Chem.*, 1996, **100**, 16502.
17 J. Riley and T. Baer, *J. Phys. Chem.*, 1993, **97**, 385.
18 N. Heinrich, F. Louage, C. Lifshitz and H. Schwarz, *J. Am. Chem. Soc.*, 1988, **110**, 8183.
19 J. A. Booze, K.-M. Weitzel and T. Baer, *J. Chem. Phys.*, 1991, **94**, 3649.
20 K.-M. Weitzel, *Int. J. Mass Spectrom. Ion Processes*, 1994, **130**, 1.
21 O. A. Mazyar and T. Baer, *J. Phys. Chem. A*, 1998, **102**, 1682.
22 G. Koster, J. M. L. Martin and C. Lifshitz, *J. Chem. Soc., Perkin Trans. 2*, 1999, **11**, 2383.
23 W. Cui, B. Hadas, B. Cao and C. Lifshitz, *J. Phys. Chem. A*, 2000, **104**, 6339; 7160.
24 L. N. Heydorn, Y. Ling, G. de Oliveira, J. M. L. Martin, C. Lifshitz and J. K. Terlouw, *Z. Phys. Chem.*, 2001, **215**, 141.
25 J. A. Montgomery Jr, M. J. Frisch, J. W. Ochterski and G. A. Petersson, *J. Chem. Phys.*, 2000, **112**, 6532.
26 R. Mitzner and E. E. B. Campbell, *J. Chem. Phys.*, 1995, **103**, 2445.
27 E. E. B. Campbell, G. Ulmer and I. V. Hertel, *Phys. Rev. Lett.*, 1991, **67**, 1986.
28 E. Kolodney, A. Budrevich and B. Tsipinyuk, *Phys. Rev. Lett.*, 1995, **74**, 510.
29 J. U. Andersen, C. Brink, P. Hvelplund, M. O. Larsson, B. Bech Nielsen and H. Shen, *Phys. Rev. Lett.*, 1996, **77**, 3991.
30 J. Lemaire, M. Heninger, R. Marx and G. Mauclaire, *Int. J. Mass Spectrom.*, 1999, **189**, 93.
31 W. A. Chupka and C. E. Klots, *Int. J. Mass Spectrom. Ion Processes*, 1997, **167/168**, 595.
32 K. Hansen and E. E. B. Campbell, *J. Chem. Phys.*, 1996, **104**, 5012.
33 J. Laskin and C. Lifshitz, *Chem. Phys. Lett.*, 1997, **277**, 564.
34 J. Laskin, B. Hadas, T. D. Märk and C. Lifshitz, *Int. J. Mass Spectrom.*, 1998, **177**, 9.
35 S. Matt, R. Parajuli, A. Stamatovic, P. Scheier, T. D. Märk, J. Laskin and C. Lifshitz, *Eur. Mass Spectrom.*, 1999, **5**, 477.
36 E. E. B. Campbell, K. Hoffmann and V. Hertel, *Eur. Phys. J. D*, submitted.
37 C. E. Klots, *Chem. Phys. Lett.*, 1991, **186**, 73.
38 P. Sandler, C. Lifshitz and C. E. Klots, *Chem. Phys. Lett.*, 1992, **200**, 445.
39 C. Lifshitz, *Int. J. Mass Spectrom.*, 2000, **198**, 1.